Model-Based Deep Learning for End-to-End Optimization in the Fiber-Terahertz Communication System

Zhongya Li(1,2), Guoqiang Li(1,2), Boyu Dong(1,2), Sizhe Xing(1,2), Jianyang Shi(1,2), Ziwei Li(1,2,3), Chao Shen(1,2,3), Nan Chi,(1,2,3) and Junwen Zhang(1,2,3) *

(1) Key Lab of EMW Information (MoE), Fudan University, Shanghai, China, 200433
(2) Shanghai ERC of LEO Satellite Communication and Applications, Shanghai CIC of LEO Satellite Communication Technology, Fudan University, Shanghai, China, 200433
(3) Peng Cheng Laboratory, Shenzhen, China, *junwenzhang@fudan.edu.cn

Abstract *We propose and experimentally demonstrate a model-based deep-learning framework that optimizes fiber-terahertz communication system end-to-end, while retaining the conventional single-carrier transceiver architecture. Jointly learning of pulse shaping, pre-equalization, digital pre-distortion, and transceivers achieves a 1.8-dB sensitivity gain and 4-Gb/s capacity improvement at 209-GHz fiber-THz system. ©2023 The Author(s)*

Introduction

Fiber-THz integration in 6G radio access networks (RAN) enables broad coverage, and ultra-reliable low-latency communications [1]. Meanwhile, AI enhances the design and optimization of 6G architectures, enabling the automation of end-to-end network optimization [2]. AI-powered RANs can adapt to network changes, optimize resources, and improve user experience [3].

The deep learning-based end-to-end (E2E) optimization scheme for communication systems interprets the transmitter, channel, and receiver as an autoencoder (AE) neural network [4]. In the AE network, the transmitter (T-ANN) and receiver annual neural networks (R-ANN) learn to design the transmitted waveform to maximize an achievable information rate (AIR) and address the channel impairment generate by the surrogate channel. This intelligent optimization technology has been proven to be superior to conventional baselines in wireless systems [5]-[7], optical fiber systems [8]-[10], and fiber-wireless systems [11]. However, the E2E schemes [5],[6],[8],[11] implicitly optimize the waveform in the "black-box" ANN incompatible with conventional communication architecture and lack practicality. The model-based approach [7] designs the T-ANN as a trainable constellation mapper combined with a trainable pulse shaping (PS) filter to explicitly interpret the optimization and preserve the architecture of a conventional single-carrier system. A similar method [10] has also been numerically evaluated in coherent WDM systems excluding amplifier nonlinearity and bit mapping optimization.

In this work, as shown in Fig. 1, we propose a model-based deep learning approach to realize bit-level E2E optimization on the fiber-THz integrated system. The E2E framework consists of several modules including a bit-to-symbol mapper, PS filter, digital pre-distortion (DPD), and receiver. The modules at the transmitter side can

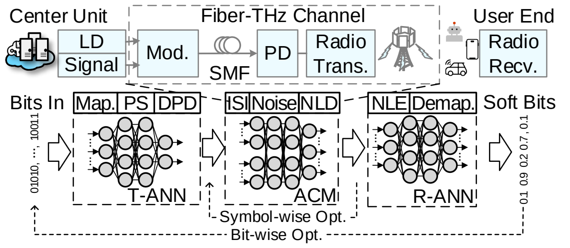

Fig. 1: Diagram of the model-based E2E optimization framework for fiber-wireless integrated system.

be directly deployed in the classic single-carrier system since the designed T-ANN has the same structure as the classic single-carrier modulation (SCM). The R-ANN can substitute all the digital signal processing (DSP) at the receiver side with significant performance enhancement compared to conventional DSPs, including a third-order Volterra nonlinear equalizer, SCM demodulation, and demapper. Experimental results indicate that our approach outperforms the conventional SCM scheme by over 1.8 dB in receiver sensitivity and 4 Gbit/s in capacity under the 20% soft-decision forward error correction (SD-FEC) bit error rate (BER) threshold (2E-2) at the 209-GHz fiber-THz integrated system.

Model-Based E2E Optimization Framework

As shown in Fig. 2(a), we designed the T-ANN to achieve the same procedures as the SCM scheme. The trainable components are in light blue. Let us denote by $\mathbf{B} \in \{0, 1\}^{K \times N}$ the matrix of bits in a transmit block which consists of N baseband symbols each carrying K bits. The bit matrix $\mathbf{B}$ is mapped into baseband symbols $\boldsymbol{s}$ by the QAM mapping module in the T-ANN. The mapping is achieved by 3 hidden layers activated with *tanh* function to produce amplitude-normalized symbols. The baseband symbols are upsampled and shaped by the PS filter. The modulated transmitted signal can be expressed as

$$x = \hat{s}_{real} * \theta_{g,real} + \hat{s}_{imag} * \theta_{g,imag} \quad (1)$$

where $\hat{s}_{real}$ and $\hat{s}_{imag}$ represent the real and imaginary part of the upsampled symbols, $\theta_{g,real}$ and $\theta_{g,imag}$ respectively represent the coefficients of the PS filter for the real and imaginary part of the symbols. To improve resistance to nonlinear distortions from the amplifiers, the modulated signal is pre-emphasized by DPD to generate the final transmit signal (Tx) as

$$x_{Tx} = tanh(x * \theta_{DPD}) + x \quad (2)$$

where θ_{DPD} denote the coefficients of a convolutional recognizer on nonlinear patterns. The DPD layer applies *tanh* activated DPD value on the modulated signal according to the recognized nonlinear pattern. The trained coefficients $\theta_{g,real}$, $\theta_{g,imag}$, and θ_{DPD} can be directly deployed in the SCM system.

In Fig. 2(b), the data-driven ANN-based channel model (ACM) also has a physics-informed structure that contains two tributaries that separately simulate the linear and nonlinear responses of the fiber-THz integrated channel. The linear tributary uses a finite impulse response (FIR) filter to simulate the channel memory effect. The nonlinear tributary uses two ResNet [12] blocks, which have a generic architecture shown in Fig. 2(d), to learn the nonlinear response of the channel. The outputs from the two tributaries are added with trainable additive Gaussian noise $\mathcal{N}(0,\theta_n)$ to get the predicted received signal (Rx).

In Fig. 2(c), the R-ANN first uses two match filters to extract the real and imaginary information from Rx and feeds the information into the demapper modules to predict the corresponding bits of the middle symbol in s. The demapper module has 2 fully-connect layers separately activated with *tanh* and *sigmoid* functions to compute soft bits. For simplicity, we make a hard decision on the output soft bits, deciding that soft bits over 0.5 are “1” and those below 0.5 are “0”.

Experimental Setup

The E2E 209 GHz fiber-THz integrated communication system is shown in Fig. 3. The system

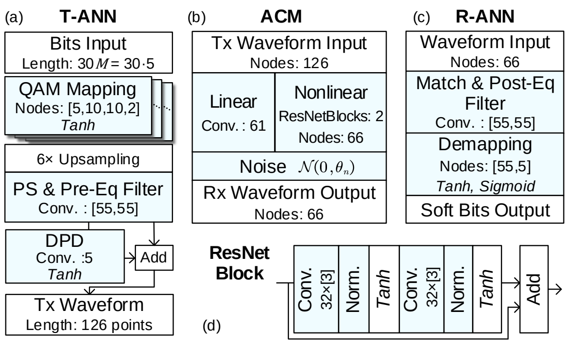

Fig. 2: Framework structure and parameters of (a) T-ANN, (b) Channel Model, (c) R-ANN and (d) ResNet block.

uses T-ANN learned coefficients to generate the Tx signal, which undergoes bit-to-symbol mapping, 6x upsampling, PS, and DPD. The Tx data is transmitted via a 64 GSa/s digital-to-analog converter (DAC), amplified by an electrical amplifier (EA), and modulates the 1550 nm light using a Mach-Zehnder modulator (MZM). The resulting optical signal is transmitted through 10 km of single-mode fiber (SMF) and detected by a photodetector (PD). An intermediate frequency signal is produced, which is then up-converted to a THz signal at 209 GHz using a second-order harmonic mixer with a 104.5 GHz local oscillator (LO). A pair of horn antennas are used for a 1-meter wireless transmission. The received THz signal is then amplified by a low-noise amplifier (LNA) and down-converted back to intermediate frequency (IF) using the second-order harmonic of the 104.5 GHz LO. The output signal is captured by an 80 GSa/s analog-to-digital converter (ADC) and decoded by the R-ANN. To account for imperfect channel modeling, 30% of the Rx and the corresponding bits data is used to fine-tune the R-ANN, while the remaining 70% is used to evaluate the performance. To encode 5 bits of information into a 32QAM SCM signal, we set K = 5 and N = 30, and the PS filter length in the T-ANN is chosen to match that of the conventional SCM baseline. Bayesian optimization algorithm [13] is used to explore other hyperparameters in the framework, and the optimized parameters appear in Fig. 2. During the training and evaluation phase, the transmitted bits are generated using different

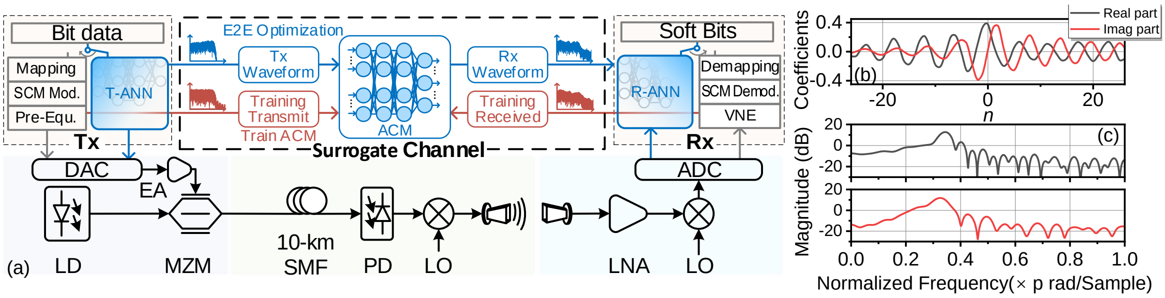

Fig. 3: (a) Experimental setup of the model-based E2E fiber-THz communication system, (b) The learned PS filter, (c) The frequency response of the PS filter.

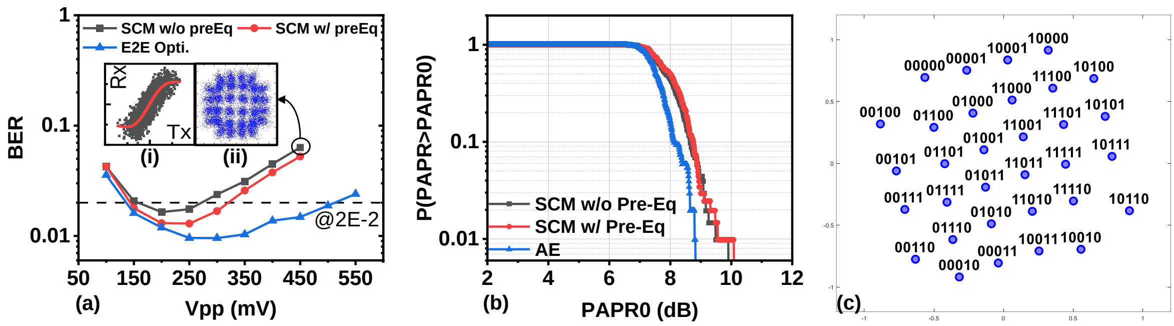

Fig. 4: (a) The BER performances of the baseline and E2E optimization schemes under different Vpp; (b) The PAPR of the T-ANN encoded signal, and SCM signals; (c) The E2E optimized bit-to-symbol constellation mapping. (i)(ii) are the AM-AM curves and the received constellations of the conventional SCM signal.

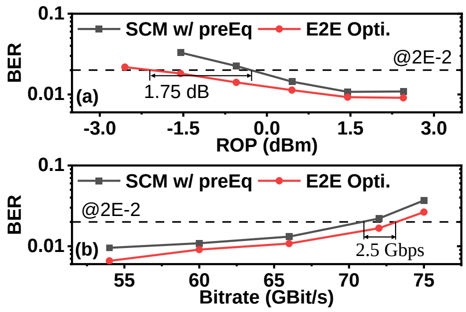

Fig. 5: The BER performances of the baseline and E2E optimization schemes under different (a) ROPs and (b) Bitrates in the BtB-wireless channel condition.

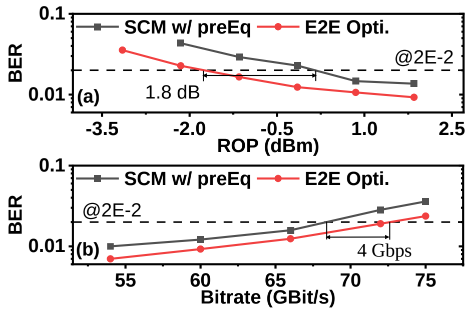

Fig. 6: The BER performances of the baseline and E2E optimization schemes under different (a) ROPs and (b) Bitrates in the 10-km fiber-wireless channel condition.

seeds to prevent the R-ANN from recognizing PRBS pattern.

The baseline conventional scheme generates 32-QAM symbols and pulse-shapes them with a square-root raised-cosine (sRRC) filter, followed by 6x upsampling to create the transmitted signal. We use additional pre-equalization (Pre-Eq) to address the fading effects present in the high-frequency band of the signal. To mitigate linear and nonlinear distortions during transmission, we use a third-order Volterra nonlinear equalizer (VNE) on the received signal [14]. After VNE, the signal is demodulated for BER calculation.

Result and Discussion

Fig. 4(b) shows that the learned PS filter ensures the orthogonality between the real and imaginary parts of the symbol. The frequency responses in Fig. 4(c) also suggest Pre-Eq ability of the filter.

We study the performance of the model-based E2E scheme in the back-to-back with wireless delivery (BtB-wireless) case and 10-km fiber-wireless transmission case. In the BtB-wireless case, Fig. 4(a) suggests the E2E scheme has strong robustness to nonlinear distortion caused by amplifiers under high signal amplitude (Vpp). The robustness is supported by the low PAPR of the final encoded Tx signal and the shaped constellation in Fig. 4(b)(c).

Fig. 5 shows the BER performance of two schemes in the BtB-wireless case, varying with ROP and bitrate. The E2E scheme outperforms the baseline, achieving a PD sensitivity gain of over 1.75 dB and a capacity improvement of 2.5 Gbit/s under the SD-FEC threshold.

Fig. 6 shows the BER performance of two schemes varying with ROP and bitrate in the fiber-wireless case. Compared to the baseline, the E2E scheme achieves a 4 Gbit/s capacity improvement in Fig. 6(a) and a 1.8 dB sensitivity gain in Fig. 6(b).

Conclusion

Our proposed approach uses model-based deep learning to optimize the fiber-THz integrated communication at the bit level, resulting in E2E performance improvements. The optimization framework, which includes the mapper, PS filter, DPD, and receiver, is jointly optimized in the E2E feedback loop. The neural transmitter ensures compatibility with SCM systems. Experimental results suggest a 1.8 dB sensitivity gain and a 4 Gbit/s capacity gain under the 20% SD-FEC threshold compare to the baseline for the 209-GHz fiber-THz system, which can be well interpreted by the optimized modules in our model-based approach.

Acknowledgment

This work is partially supported by National Key Research and Development Program of China (2022YFB2903600), NNSF of China (62235005, 62171137, 61925104), NSF of Shanghai (21ZR1408700), and the Major Key Project PCL.

References

[1] H. Tataria, M. Shafi, A. F. Molisch, M. Dohler, H. Sjöland, and F. Tufvesson, "6G Wireless Systems: Vision, Requirements, Challenges, Insights, and Opportunities," *Proceedings of the IEEE*, vol. 109, no. 7, pp. 1166–1199, Jul. 2021, DOI: 10.1109/JPROC.2021.3061701.

[2] L. Bonati, S. D'Oro, M. Polese, S. Basagni, and T. Melodia, "Intelligence and Learning in O-RAN for Data-Driven NextG Cellular Networks," *IEEE Communications Magazine*, vol. 59, no. 10, pp. 21–27, Oct. 2021, DOI: 10.1109/MCOM.101.2001120.

[3] ORAN Alliance, "O-RAN: Towards an open and smart RAN." 2018. [Online]. Available: https://www.o-ran.org/resources.

[4] T. O'Shea and J. Hoydis, "An Introduction to Deep Learning for the Physical Layer," *IEEE Transactions on Cognitive Communications and Networking*, vol. 3, no. 4, pp. 563–575, 2017, DOI: 10.1109/TCCN.2017.2758370.

[5] B. Zhu, J. Wang, L. He, and J. Song, "Joint Transceiver Optimization for Wireless Communication PHY Using Neural Network," *IEEE Journal on Selected Areas in Communications*, vol. 37, no. 6, pp. 1364–1373, Jun. 2019, DOI: 10.1109/JSAC.2019.2904361.

[6] M. Lu, B. Zhou, and Z. Bu, "Attention-Empowered Residual Autoencoder for End-to-End Communication Systems," *IEEE Communications Letters*, pp. 1–1, 2023, DOI: 10.1109/LCOMM.2023.3242281.

[7] F. Ait Aoudia and J. Hoydis, "Waveform Learning for Next-Generation Wireless Communication Systems," *IEEE Transactions on Communications*, vol. 70, no. 6, pp. 3804–3817, Jun. 2022, DOI: 10.1109/TCOMM.2022.3164060.

[8] B. Karanov, M. Chagnon, F. Thouin, T. A. Erikssonet, H. Bulow, D. Lavery, P. Bayvel, L. Schmalen, "End-to-End Deep Learning of Optical Fiber Communications," *Journal of Lightwave Technology*, vol. 36, no. 20, pp. 4843–4855, 2018, DOI: 10.1109/JLT.2018.2865109.

[9] B. Karanov, D. Lavery, P. Bayvel, and L. Schmalen, "End-to-end optimized transmission over dispersive intensity-modulated channels using bidirectional recurrent neural networks," *Optics Express*, vol. 27, no. 14, p. 19650, Jul. 2019, DOI: 10.1364/OE.27.019650.

[10] J. Song, C. Hager, J. Schroder, A. G. I. Amat, and H. Wymeersch, "Model-Based End-to-End Learning for WDM Systems With Transceiver Hardware Impairments," *IEEE Journal of Selected Topics in Quantum Electronics*, vol. 28, no. 4, p. 14, 2022, DOI: 10.1109/JSTQE.2022.3163474.

[11] Z. Li, J. Jia, G. Li, B. Dong, W. Shen, C. Huang, J. Shi, N. Chi, and J. Zhang, "Deep-learning-based multi-user framework for end-to-end fiber-MMW communications," Optics Express, vol. 31, no. 10, pp. 15239–15255, May 2023, DOI: 10.1364/OE.479500.

[12] K. He, X. Zhang, S. Ren, and J. Sun, "Deep Residual Learning for Image Recognition," in *2016 IEEE Conference on Computer Vision and Pattern Recognition (CVPR)*, Jun. 2016, pp. 770–778. DOI: 10.1109/CVPR.2016.90.

[13] B. Shahriari, K. Swersky, Z. Wang, R. P. Adams, and N. de Freitas, "Taking the Human Out of the Loop: A Review of Bayesian Optimization," *Proceedings of the IEEE*, vol. 104, no. 1, pp. 148–175, Jan. 2016, DOI: 10.1109/JPROC.2015.2494218.

[14] N. Stojanovic, F. Karinou, Z. Qiang, and C. Prodaniuc, "Volterra and Wiener Equalizers for Short-Reach 100G PAM-4 Applications," *Journal of Lightwave Technology*, vol. 35, no. 21, pp. 4583–4594, 2017, DOI: 10.1109/JLT.2017.2752363.